The electrochemistry of pyrite in chloride solutions

Michael Nicol, Suchun Zhang, Venny Tjandrawan

PII: S0304-386X(18)30027-6
DOI: doi:10.1016/j.hydromet.2018.04.013
Reference: HYDROM 4802

To appear in: *Hydrometallurgy*

Received date: 9 January 2018
Revised date: 19 February 2018
Accepted date: 16 April 2018

Please cite this article as: Michael Nicol, Suchun Zhang, Venny Tjandrawan , The electrochemistry of pyrite in chloride solutions. The address for the corresponding author was captured as affiliation for all authors. Please check if appropriate. Hydrom(2018), doi:10.1016/j.hydromet.2018.04.013

The Electrochemistry of Pyrite in Chloride Solutions

Michael Nicol*, Suchun Zhang, Venny Tjandrawan

School of Engineering and Information Technology and Energy, Murdoch University, Perth,

WA 6150, Australia

*Corresponding author.

Abstract

A detailed study of the anodic and cathodic behaviour of natural pyrite in acidic chloride solutions containing various oxidants has been conducted as part of an overall program on the fundamental aspects of the heap leaching of copper sulphide minerals.

The stoichiometry of the anodic dissolution reaction depends on the potential in that it varies from less than 4F/mole Fe dissolved at potentials below 0.8V(SHE) to 15F/mole Fe at potentials above about 1.0V(SHE).

The mixed potentials of pyrite in chloride solutions containing iron(III) are greater than those in the presence of copper(II) and both increase with agitation as a result of enhanced transport of iron(II) and copper(I) from the surface of the dissolving mineral. The mixed potentials are unaffected by the presence of dissolved oxygen confirming the low reactivity for the cathodic reduction of oxygen.

The rate of anodic dissolution of pyrite in chloride solutions is independent of the acid and chloride concentration except at high chloride concentrations when the rate decreases slightly. The potential dependence of the anodic reaction roughly follows Tafel behaviour up to about 1.0V but mechanistic conclusions are excluded due to the variable stoichiometry.

Cathodic reduction of oxygen is some 30 times slower than that of 1 g/L iron(III). The reduction of copper(II) is also less significant in the leaching of pyrite due to the lower formal potential of the copper(II)/copper(I) couple than that of the iron(III)/iron(II) couple in concentrated chloride solutions.

Comparative measurements have shown that pyrite will dissolve more slowly than chalcopyrite in chloride solutions and, this coupled to the low sulfate yield at low potentials, suggests that oxidation of pyrite as a source of heat in abiotic heap leaching is unlikely.

Key words: Pyrite; dissolution, chloride;iron(III);copper(II)

1.Introduction

The recovery of copper by heap leaching of low-grade ores containing secondary and tertiary copper sulfide minerals is becoming increasingly important as the easily leached oxide ores are being depleted.

Although it is well known that the rate of leaching of the secondary copper sulfides is more rapid than that of the primary minerals such as chalcopyrite and enargite under strongly oxidizing conditions, the rates are considerably slower than those for the most common oxide minerals. In addition, an oxidant is required for the sulfides and bacterially-assisted oxidation in sulfate solutions has been the generally accepted method for heap leaching of such minerals. An alternative approach using dilute chloride solutions has been applied in at least one case (Aroca, 1999) and more concentrated chloride solutions are currently being used in an operation in northern Chile. Chloride is an attractive alternative which can also make use of copper(II) as an oxidant. The rapid (relative to that of iron(II)) rate of the re-oxidation of copper(I) by dissolved oxygen in chloride solutions (Miki and Nicol, 2008a, 2011) permits the use of aerated heaps without external regeneration of the oxidant.

Pyrite commonly occurs with the copper sulfide minerals and can potentially also be leached during chloride leaching. This can be a disadvantage in terms of higher oxygen demand and higher iron concentrations in the pregnant leach solutions. On the other hand, oxidation of pyrite has the potential to generate heat in the heaps thereby increasing the rate of leaching of the copper minerals. It was therefore considered important to undertake an electrochemical study of the behaviour of pyrite under chloride leaching conditions. A similar electrochemical study aimed at bacterial leaching of copper sulfides in sulfate media has previously been published (Nicol et al, 2013).

Although there have been many published reports on the electrochemistry of pyrite in both sulfate and chloride media (Peters and Majime, 1968; Biegler et al., 1975; Biegler and Swift, 1979; Misra and Osseoasare, 1988, 1992; Zhu et al, 1993; Kelsall et al., 1996; Ahlberg and Broo, 1997; Lin and Say, 1997; Lehmann et al, 2000; Nicol and Liu, 2003; Rimstidt and Vaughan, 2003; Antonijevic et al, 2005; Lehner et al, 2007; Miki and Nicol, 2008; Bryson and Crundwell, 2014; Lin et al, 2014; Nicol et al, 2016;), none of these have addressed in any detail the electrochemistry under conditions appropriate to the heap leaching of pyrite under chloride conditions. In a detailed electrochemical study (Holmes and Crundwell, 2000) presented useful information on the electrochemistry of pyrite under various conditions in sulfate solutions at low temperatures and the authors developed a conventional mixed-potential model for the oxidative dissolution of pyrite in sulfate solutions containing iron(III), iron(II) and dissolved oxygen which correlated well with the observed electrochemical data. In a subsequent paper (Bryson and Crundwell, 2014), the same authors treated similiar electrochemical data obtained in hydrochloric acid solutions in terms of the semi-conducting properties of pyrite. However, their data is of limited value as it was focussed on results at potentials higher than would be

experienced by pyrite under heap leach conditions. The same considerations in terms of the potential region investigated apply to the other studies (Lehmann et al, 2000; Lin et al, 2014) conducted in chloride solutions.

This paper presents the results of a study of the anodic and cathodic electrochemistry of pyrite over a wide range of chloride concentrations at potentials relevant to the dissolution of the mineral under ambient conditions appropriate to heap leaching.

2. Experimental

The properties of the natural pyrite samples and fabrication into electrodes have been described in a previous publication (Nicol et al, 2013). The electrodes prepared with a normal cubic face exposed to the solution are labelled "pyrite1" and "pyrite3" while that with the diagonal face exposed is "pyrite2". A fourth electrode, "pyrite4" was prepared from a local musuem-grade single crystal with the cubic face exposed. The counter electrode was a thin, coiled platinum (Pt) wire of about 10 cm in length housed in a tube with a fritted glass end to isolate the solution from that in the cell. The reference electrode was either a mercury-mercurous chloride (sat. KCl) electrode with a potential of 0.254 V against the standard hydrogen electrode (SHE) at 25°C or a silver-silver chloride (3MKCl) electrode with a potential of 0.210 V versus SHE at 20°C. All potentials in this study have been reported against SHE.

Details of the conventional electrochemical methods and experimental procedures have been provided in a previous publication (Nicol et al., 2016). As previously described, electrochemical measurements were carried out using a standard three-electrode system with one of the above pyrite electrodes used as a rotating (100 to 500 rev/min) working electrode.

The above three-electrode system was used in conjunction with either a EG & G Princeton Applied Research Model 173 Potentiostat / Galvanostat and an EG & G Princeton Applied Research Model 175 Universal programmer or a Solartron 1720 potentiostat to conduct the electrochemical measurements. Current and potential readings from the former were captured using a National Instrument data acquisition card, which was controlled by Labview™ software while CorrWare software was used with the latter potentiostat.

The solutions used as electrolytes in this study were all prepared using analytical grade (AR) chemicals and Millipore-quality (Milli-Q) water.

Prior to each experiment, the electrode surfaces were very gently sanded with P1200 silicon carbide paper for a few seconds. Thereafter, the mineral was wet-polished in the same way using a finer grind (4000 grit) silicon carbide paper. Experiments were conducted at either 25°C or 35°C.

Analysis of iron in solution was conducted colorimetrically at 515 nm using the o-phenanthroline method (Vogel, 1961) in the presence of hydroxlamine to reduce any iron(III) to iron(II).

3. Results and Discussion

3.1 Thermodynamic Considerations

It is known that pyrite can be oxidised in acid solutions to form either/or both sulfur and sulfate ions. The stoichiometry will be dealt with in a later section.

The overall oxidative dissolution of pyrite with iron(III) as the oxidant can be written as

$$FeS_2 + 2Fe^{3+} \rightarrow 3Fe^{2+} + 2S° \quad (1)$$

$$FeS_2 + 8H_2O + 14\,Fe^{3+} = 15Fe^{2+} + 2HSO_4^- + 14H^+ \quad (2)$$

Oxidation can also be accomplished with copper(II) ions as the oxidant in chloride solution

$$FeS_2 + 2Cu(II) \rightarrow Fe(II) + 2Cu(I) + 2S° \quad (3)$$

The potentials for the oxidation of pyrite in a solution of 4M chloride containing 0.05 M iron(II) , 0.1M H^+ and 0.1M HSO_4^- can be calculated using the Nernst equation and the standard electrode potentials (HSC Chemistry, Ver 7.1) as

$$FeS_2 = Fe^{2+} + 2S + 2e \qquad E_o = 0.352V \quad (4)$$

$$FeS_2 + 8H_2O = Fe^{2+} + 2HSO_4^- + 14H^+ + 14e \qquad E_o = 0.267V \quad (5)$$

These values have been calculated ignoring the weak complexation of iron(II) by either sulfate or chloride ions.

The formal potential of the iron(III)/iron(II) couple decreases from 0.740V in the absence of chloride to 0.693V in 4M chloride while that of the copper(II)/copper(I) couple varies from 0.390V in 0.1M chloride to 0.572V in 4M chloride (Nicol et al, 2016).

Given that the potentials for the iron(III)/iron(II) couple are 0.3 to 0.4V greater than those for reactions (4) and (5), there are no thermodynamic restrictions to the oxidation of pyrite by iron(III) with either sulfur or bisulfate as the oxidation products. In the case of copper(II) as the oxidant, this is also true at high chloride concentrations but not at low chloride concentrations except at high copper(II)/copper(I) concentration ratios.

3.2 Mixed Potential Measurements.

Mixed potential measurements were made under various conditions by immersing the electrode in the relevant solution for up to 30 min under open-circuit conditions. These measurements provide information on the potential regions relevant to leaching and also a preliminary indication of the effectiveness of the oxidants. The effect of mass transport was evaluated by initially measuring the potential of a stationary electrode for a period after which the electrode

was rotated at 500 rev/min. These measurements were made in solutions of various chloride concentrations and pH but only the data obtained in 1 M HCl solutions are shown below.

The results in the absence of an oxidant and in the presence of dissolved oxygen (solution sparged with pure oxygen) are shown in Fig. 1 from which it is apparent that the mixed potential is some 40 mV greater in the presence of oxygen suggesting that dissolved oxygen does act as an oxidant in this system. No effect of agitation was observed with oxygen as could be expected given the low reactivity of oxygen. This is confirmed by comparing the mixed potential of about 0.58V with oxygen with those measured in solutions containing iron(III) and copper(II) in Fig. 2 and Fig. 3 that are significantly greater. The small increase in the potential with agitation in the case of the solution sparged with nitrogen is probably due to the entrainment of some oxygen from the air during agitation.

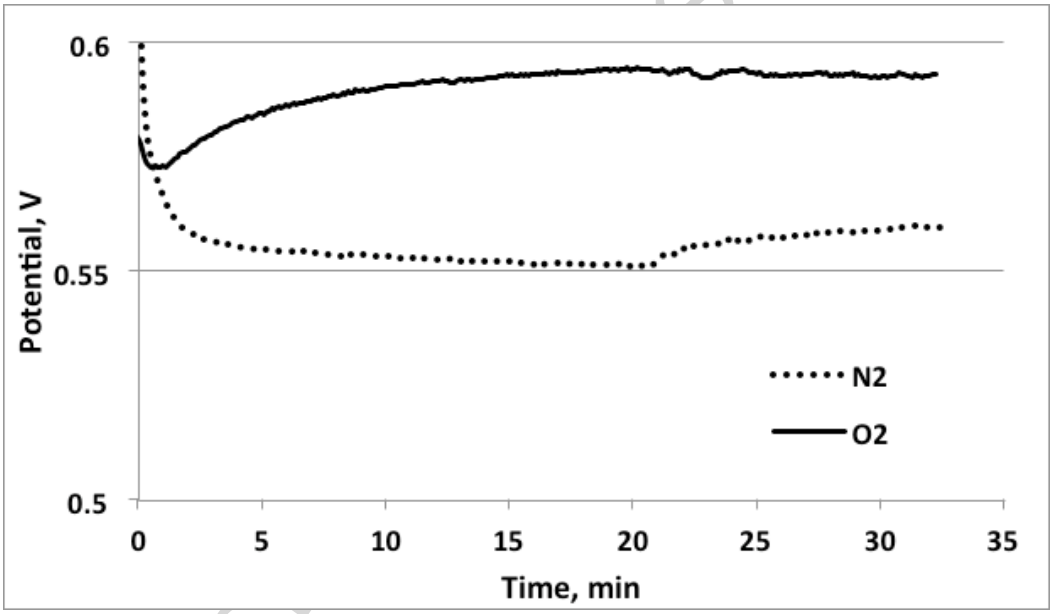

Fig.1 Open circuit potential transients for a stationary pyrite1 electrode in a solution of 1 M HCl at 35ºC. After 20 min, the electrode was rotated at 500 rev/min

The mixed potentials in solutions containing 1 g/L of either iron(III) or copper(II) are shown in Fig. 2 and Fig. 3. The potential is higher in the presence of iron(III) than copper(II) as expected given the higher formal potential of the former. In a solution containing both oxidants (Fig. 4), the potentials are similar to those with only iron(III) present i.e. the rate of dissolution is measurably greater with iron(III) than copper(II) as the oxidant. Note that, in all cases, the results are similar in solutions sparged with either nitrogen or oxygen confirming the above conclusion about the low reactivity of oxygen. In all cases, the mixed potential increased on agitation. This is not due to increased mass transport of the oxidants to the surface but increased mass transport of the reduced species (iron(II) and copper(I)) from the surface. Thus, as shown in reactions 1, 2

and 3, the concentrations of either iron(II) or copper(I) increase at the surface of the pyrite due to dissolution under open-circuit conditions. This results in a decrease in the potential at the surface. However, the surface concentration will decrease with increasing mass transport of these species from the surface resulting in an increase in potential with agitation. This will be dealt with in more detail in a later section

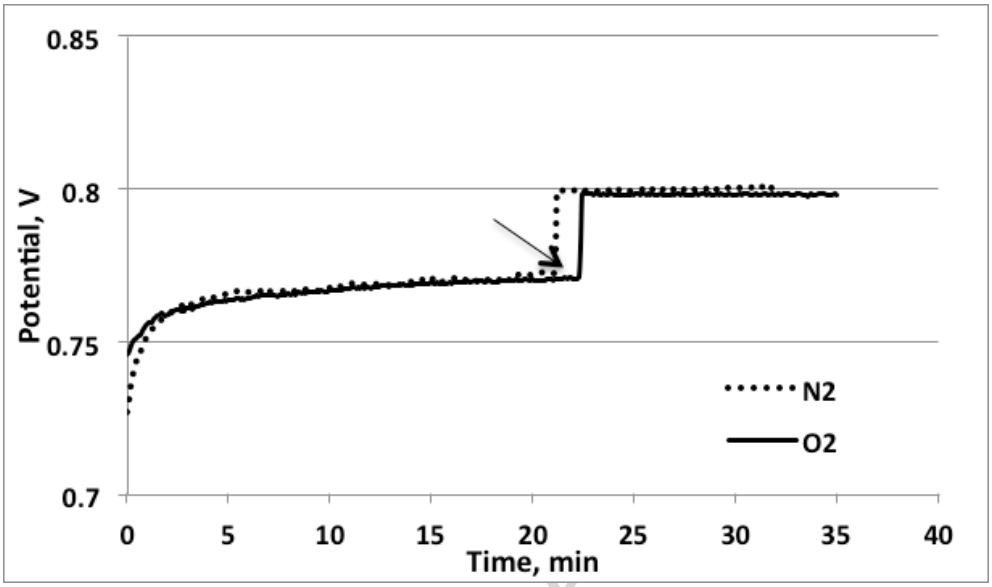

Fig. 2 Potential transients for a stationary pyrite1 electrode in a solution of 1 M HCl + 1 g/L iron(III) at 35°C. At the point indicated, the electrode was rotated at 500 rev/min.

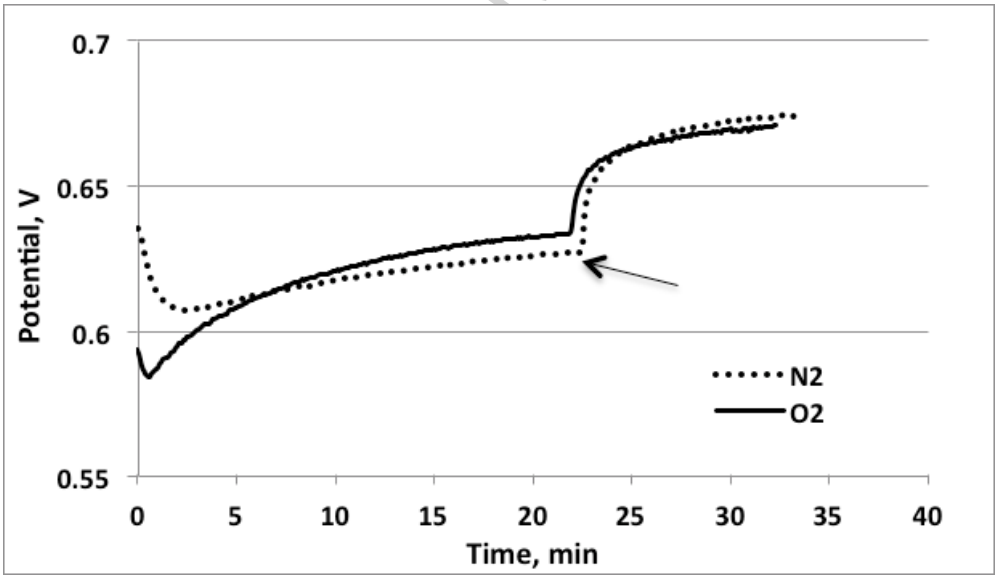

Fig. 3 Potential transients for a stationary pyrite1 electrode in a solution of 1 M HCl + 1 g/L copper(II) at 35°C. At the point indicated, the electrode was rotated at 500 rev/min.

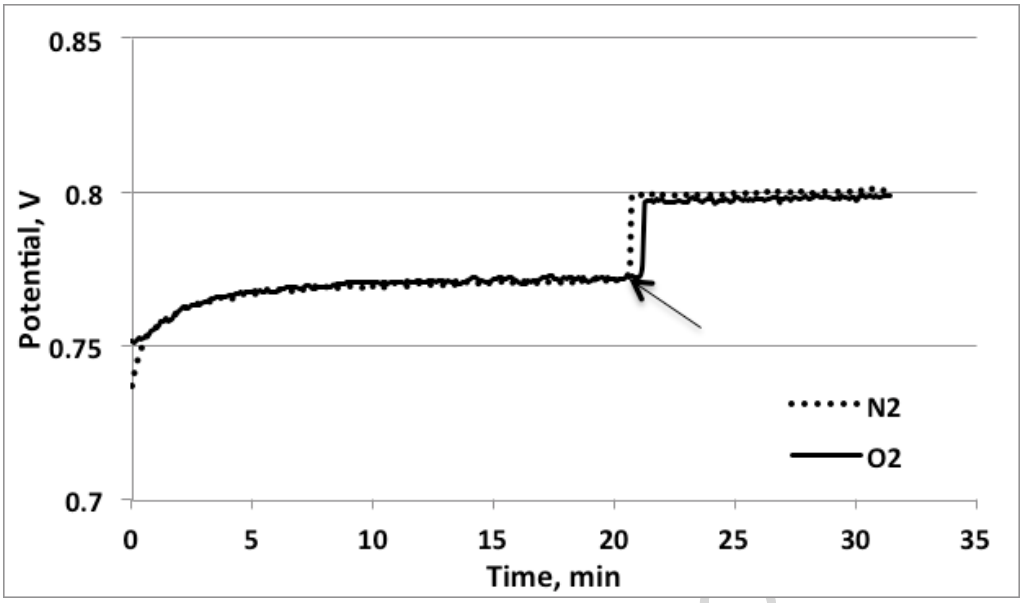

Fig. 4 Potential transients for a stationary pyrite1 electrode in a solution of 1 M HCl + 1 g/L iron(III) + 1 g/L copper(II) at 35°C. At the point indicated, the electrode was rotated at 500 rev/min.

3.3 Anodic Oxidation.

The mixed potential measurements have shown that further electrochemical experiments should focus on the potential range between about 0.55 V and 0.85 V as being relevant to dissolution. Thus, Fig. 5 shows a typical slow sweep voltammogram that was obtained by sweeping the potential applied to a rotating electrode in a positive direction from the rest potential at about 0.6V in a concentrated chloride solution. The small peak at about 0.7V precedes significant dissolution that only occurs at potentials above about 0.8V. The cathodic peak at 0.65V is probably associated with reduction of the surface species formed during the positive sweep. Soluble intermediates associated with the peak at 0.7V would not be present at the rotating electrode surface during the negative sweep. The surface species responsible for these complementary peaks is not known at this stage.

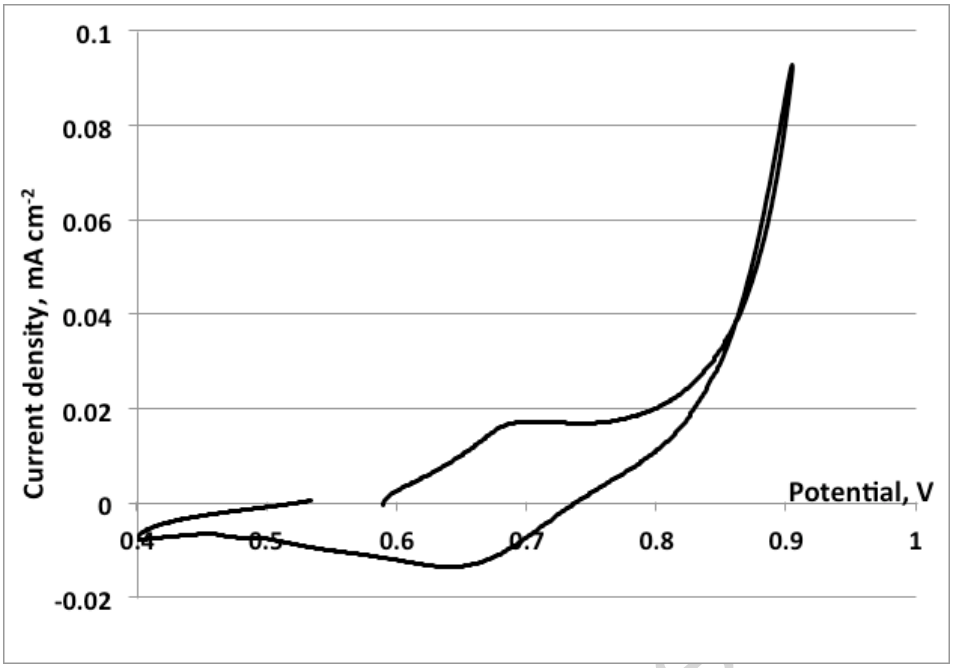

Fig. 5 Cyclic voltammogram (1 mV/s) for a rotating pyrite1 electrode in a solution of 4M NaCl + 0.02M HCl at 25°C. The sweep was initiated in a positive direction from the rest potential at 0.59V.

The stoichiometry of anodic dissolution was studied by analysing the solutions for dissolved iron after potentiostatic oxidation at various potentials for various times from 1h to 5h in 1MHCl. The results are summarized in Fig. 6 as the number of Faradays of charge/mol Fe dissolved.

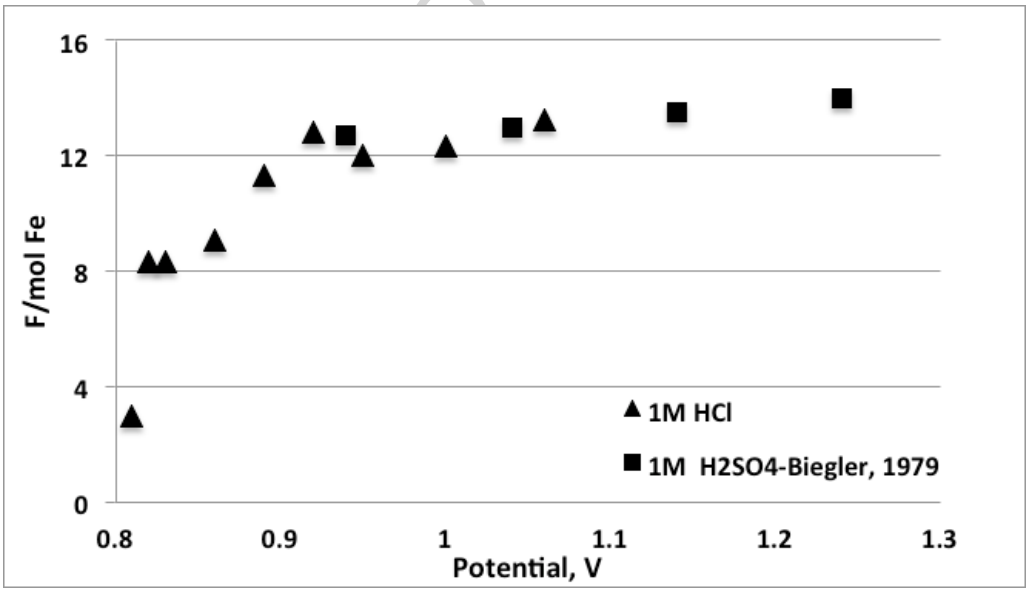

Fig. 6 Coulometric analysis of the anodic dissolution of pyrite4 in 1M HCl solution at 25°C. Also shown is the data (Biegler and Swift, 1979) in 1M H_2SO_4 solution.

These results confirm those previously published (Biegler and Swift, 1979) that, at high potentials (greater than 0.9V), the stoichiometry approaches that of reaction (5) of 14 e/Fe (or 15e/Fe with iron(III) as the product). However, at lower potentials relevant to this study, the

values obtained suggest that oxidation of sulfide to sulfate is not complete. While there is some uncertainty for the point at the lowest potential due to the low concentration of iron in solution, the values around 8 e/Fe are reliable having been confirmed by ICP analysis of some of the solutions for iron. These results suggest that either reactions (4) and (5) occur to varying extents in parallel or that a reaction such as

$$FeS_2 + 3H_2O = Fe^{2+} + S_2O_3^{2-} + 6H^+ + 6e \qquad (6)$$

is also involved in the low potential region. Possible evidence for the involvement of an oxidisable intermediate sulfur species was observed in attempts to distinguish between iron(II) and iron(III) in the colorimetric analysis. Thus, iron(III) can also be determined from the absorbance at 396 nm in solutions without the addition of hydroxylamine. In attempting this, it was observed that the absorbance slowly (over a period of about 30 min) increased at 515 nm due presumably to slow reduction of iron(III) by a species such as thiosulfate in the solution after anodic oxidation.

These results of variable stoichiometry make quantitative interpretation of the anodic dissolution current/potential relationships uncertain as will be discussed below.

Potentiostatic measurements were made by intially holding the potential at 0.7V for 20 min. and recording the current as a function of time. The potential was increased in 50mV increments and the current-time transients recorded after each increase in potential. The results obtained in a 3M NaCl solution are shown in Fig. 7.

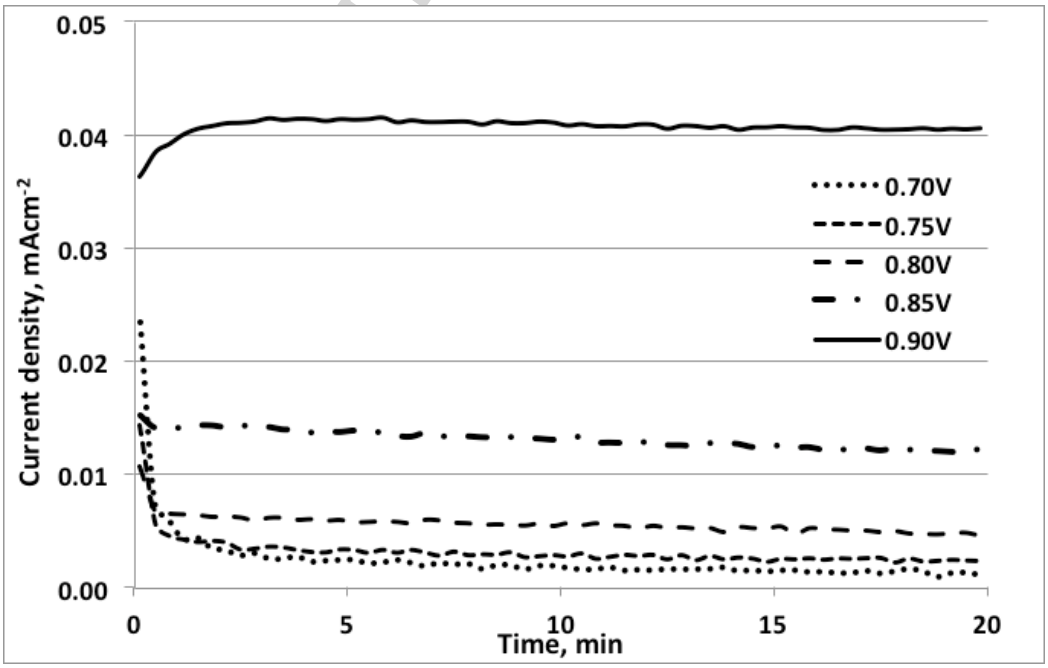

Fig. 7 Potentiostatic current-time transients for the anodic oxidation of a rotating (200rev/min) pyrite4 electrode in a solution of 3M NaCl + 0.01M HCl at 25°C.

As expected, the currents increase with increasing potential and approach steady-state values after 20 min. Similar results were obtained in a solution with the same total chloride concentration but higher acidity. The current densities measured after 20 min are plotted as Tafel curves in Fig. 8 for all solutions having a total chloride concentration of 3M. There is little difference in the curves at the different acidities confirming previously published data (Bryson and Crundwell, 2014) that the proton is not involved in the rate-determining step. The Tafel plots are non-linear with increasing slopes at higher potentials. This is possibly due to the changing stoichiometry with the ratio e/Fe increasing with potential and highlights the problem in deriving a suitable slope for the curves. It is also a simple chemical explanation for variable Tafel slopes previously attributed to semiconductor effects (Bryson and Crundwell, 2014) in which experiments these authors also did not allow for uncompensated resistance at high current densities. At the low currents observed at potentials below 0.95V in this study, the iR drops were found to be negligible.

The effect of the chloride concentration on the anodic dissolution is shown in Fig. 9 from which it is apparent that there are not significant differences between 1M and 4M NaCl solutions.

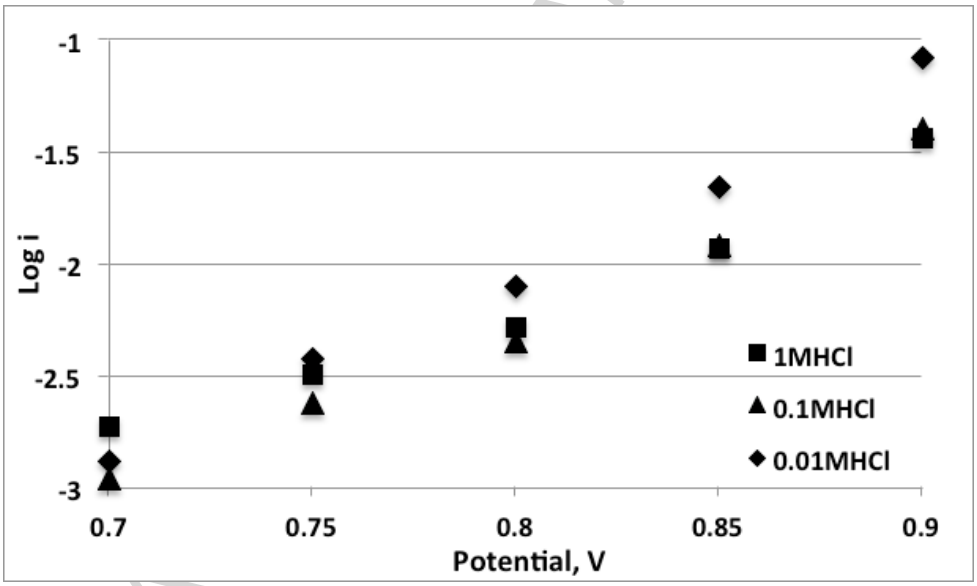

Fig. 8 Tafel plots for the anodic currents after 20 min at various potentials for a rotating (200 rev/min) pyrite4 electrode in solutions of 3M total chloride at 25ºC.

The larger peaks in the 1M case should not be considered indicative of differences in behaviour due to the chloride concentration as it was found that the magnitude of the peaks was variable and could depend on, for example, the surface preparation and extent of oxidation during the open-circuit period preceding the sweep in the positive direction.

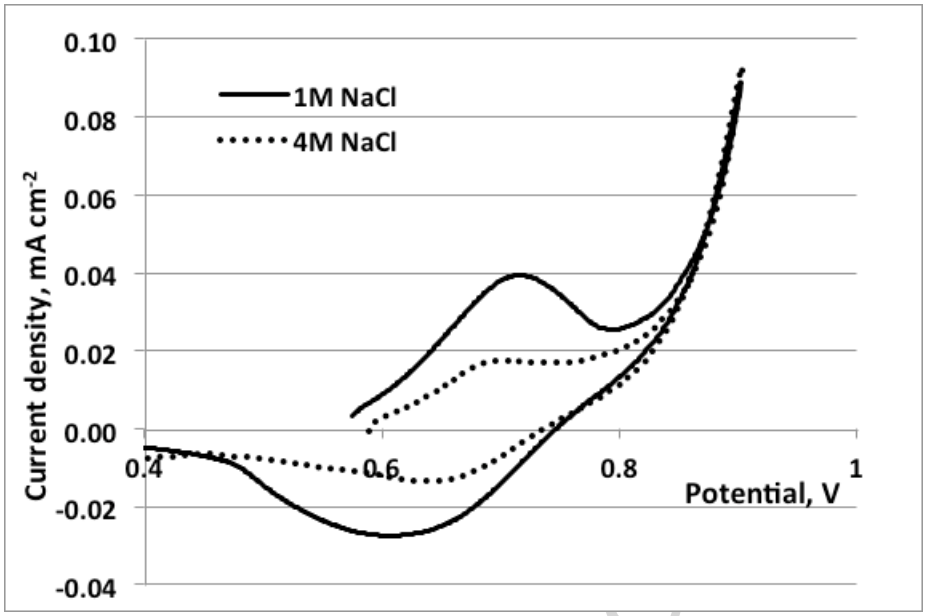

Fig. 9 Cyclic voltammograms (1 mV/s) for the anodic oxidation of a rotating (200rev/min) pyrite1 electrode in solutions of 1M and 4M NaCl with 0.02M HCl at 25ºC.

These results agree with published data that showed no effect of chloride between 0.25M and 1.0M (Bryson and Crundwell, 2014) at potentials up to 1.4V.

Steady-state currents at various potentials in solutions of increasing chloride concentation at low pH are shown in Fig. 10 from which it is apparent that the chloride concentration has little effect up to 2M but the reactivity is reduced at 4M total chloride. It is interesting to note that very similar data was obtained in 1M sulfuric acid solution. This suggests that the rate of leaching of pyrite could be expected to be similar in chloride and sulphate solutions.

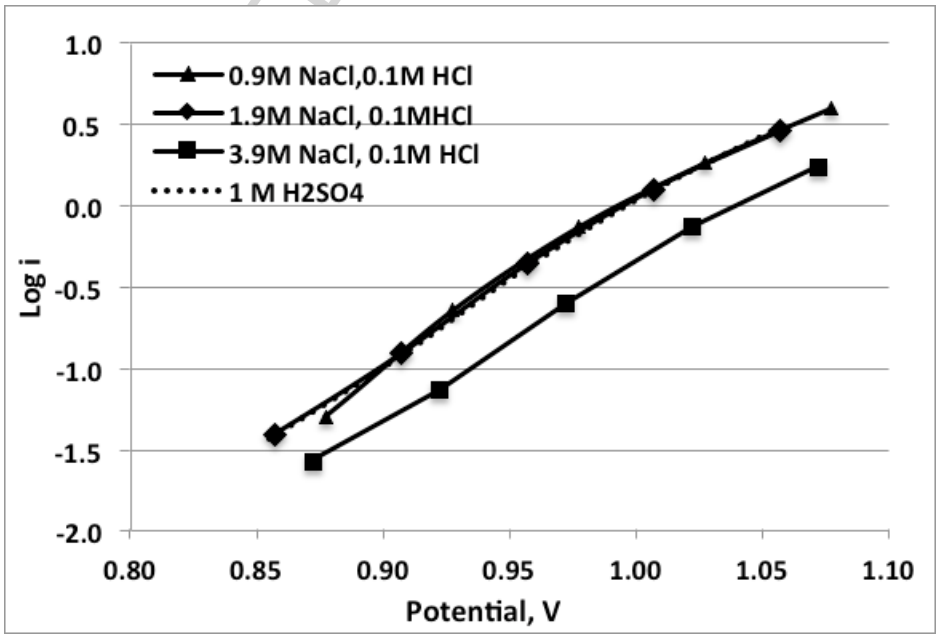

Fig. 10 Tafel plots for the anodic currents after 20 min at various potentials for a rotating (200 rev/min) pyrite2 electrode in solutions of various chloride concentration at 25°C. Also shown is the curve obtained in 1MH_2SO_4 solution.

The shape of the current-time transients shown in Fig. 7 were generally observed in solutions of low pH. They are characterized by falling currents that stabilize after about 20-30min. In solutions of high chloride concentration at higher pH values, the transients exhibited the same shape at potentials below about 1.0v but, as shown in Fig. 11, the transient obtained at 1.0V is different and the current density after 1h is substantially greater than the values at lower potentials. This behaviour was not reproducible and could be associated with variable surface preparation of the electrode. The shape of the transient is similar to that expected for the nucleation and growth of a phase on the electrode surface.

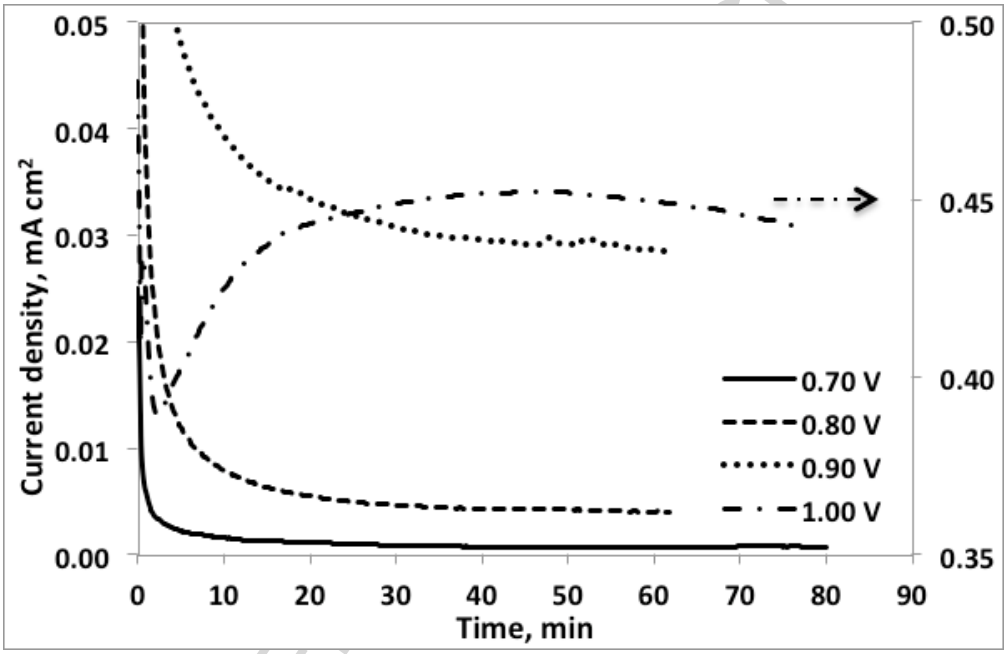

Fig. 11. Potentiostatic current-time transients for a rotating (100 rev/min) pyrite1 electrode at various potentials in a solution of 4M NaCl at a pH of 1.1 at 25°C.

Pseudo-steady-state potentiostatic measurements in which the current after 1h at various potentials in concentrated sodium chloride solution was measured are summarized in Fig. 12.

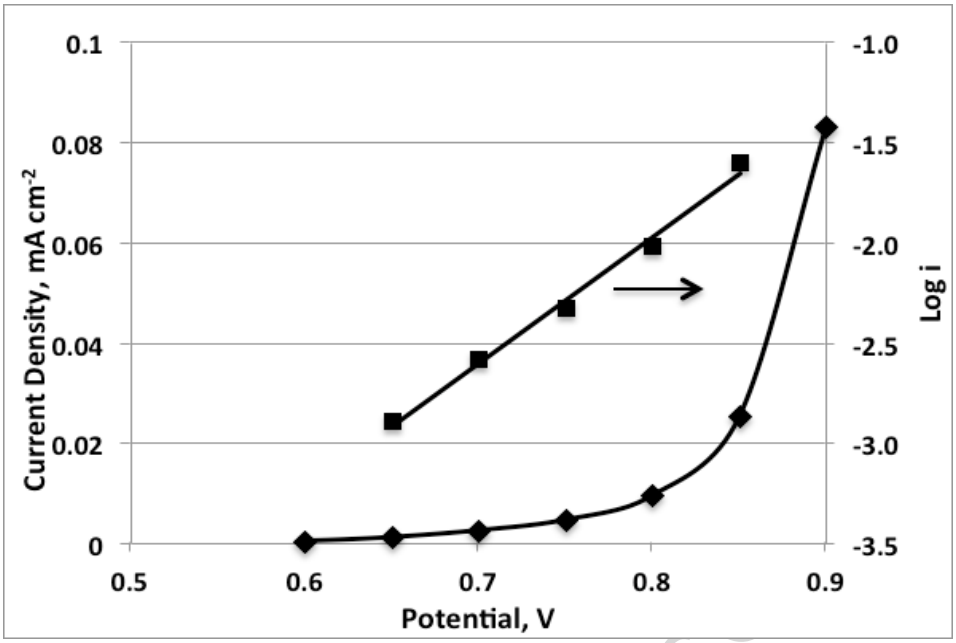

Fig. 12. Pseudo-steady-state current as a function of potential for a rotating (100 rev/min) pyrite2 electrode in a solution of 4M NaCl + 0.02MHCl under nitrogen at 25^{o}C as linear and logarithmic plots.

These results confirm those in Fig. 10 that approximately linear Tafel plots with a slope of about 150mV/decade are obtained at potentials below 1.0V. Because of the varying stoichiometry of the anodic dissolution reaction, no mechanistic conclusions based on the magnitude of this slope can be justified.

The effect of the source of the pyrite on its anodic reactivity is shown in Fig. 13 as steady-state current/potential curves for each of the four pyrite electrodes. There is relatively little variation in reactivity under these conditions for these electrodes that consisted of pyrite from two sources and with different crystal faces exposed. If semiconducting properties are important in determining anodic reactivity, one could have expected greater differences between the four electrodes.

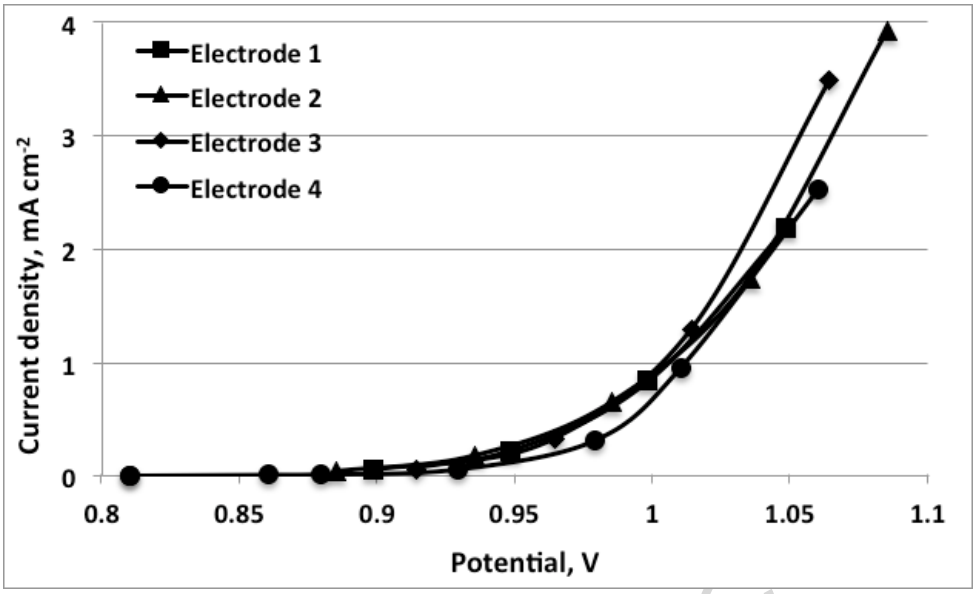

Fig. 13. Steady-state current potential curves for various pyrite electrodes in 1 M HCl at 25ºC.

3.4. Cathodic Processes

The cathodic reduction of dissolved oxygen was studied using slow-sweep voltammetry after the open-circuit potential measurements shown in Fig. 1. The results are shown in Fig. 14. The greater cathodic currents observed at potentials below about 0.5V in the solution saturated with oxygen are due to the reduction of dissolved oxygen. There is a small amount of hysteresis on the reverse sweep from 0.3V in both cases.

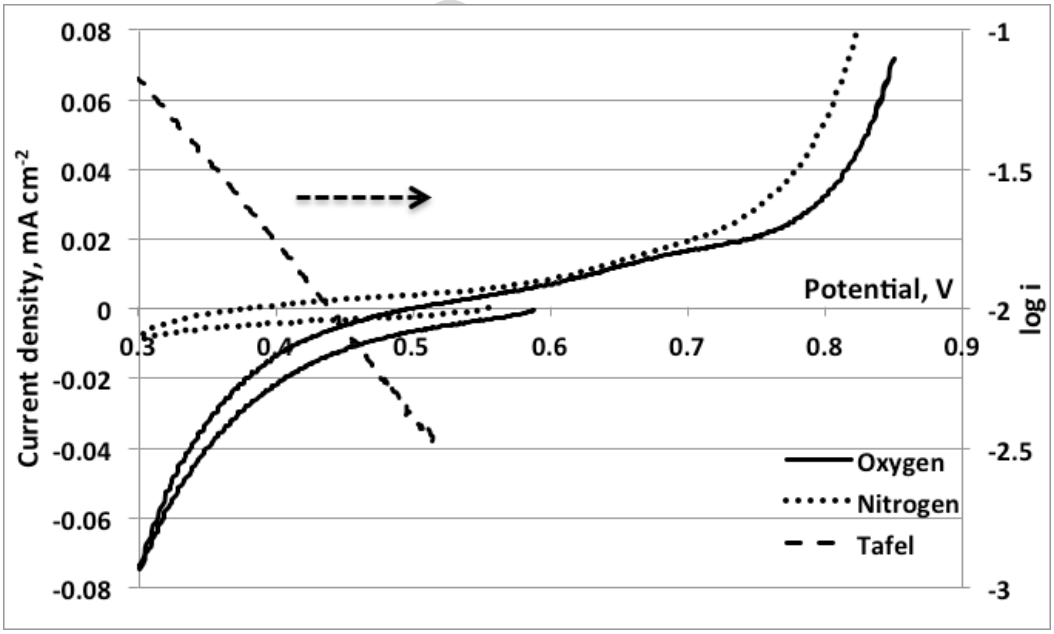

Fig.14. Cyclic voltammograms for a rotating (500 rev/min) pyrite1 electrode at 1 mV/s in a solution of 1M HCl at 35ºC. The sweeps were initiated in a negative direction after 30 minutes at the rest potentials. Also shown is the Tafel plot for reduction of oxygen.

Subtraction of the "background" current obtained under nitrogen from that obtained in oxygen allows the current due to oxygen reduction to be obtained (using the data for the positive-going

branch). This plotted as a Tafel relationship in Fig. 14 that demonstrates linear behaviour with a Tafel slope of 160 mV/decade. This is in agreement with the value of 141mV/decade obtained in 0.1M perchloric acid. (Biegler et al, 1975). Extrapolation of the Tafel line to the mixed potential of 0.59V gives a current density of 0.0012 mA cm^{-2} for the rate of dissolution (1e-basis). This will be compared with the rate in the presence of iron(III) below.

The reduction of iron(III) and copper(II) was studied using cyclic voltammetry and the main features at several concentrations are summarized in Fig. 15 for deaerated 4M NaCl solutions.
As expected from the formal and mixed potentials (Fig.2 and 3), iron(III) is reduced at more positive potentials than copper(II) and the curves for both oxidants have a typical S-shape with limiting current densities at potentials below about 0.4V. The current densities are proportional to the concentrations with copper(II) having greater limiting currents than iron(III) due to the greater diffusion coefficient of the former (Nicol et al, 2016). Current densities for a mixture of both metal ions is the sum of the current densities for the individual species. Reduction of copper(II) on a platinum electrode is slightly faster than on pyrite at potentials below the limiting current. As suggested by the similarity of the mixed potentials in these solutions (Figs. 2, 3 and 4), the curves were the same in the presence or absence of dissolved oxygen at potentials above about 0.5V as also could be expected from the data in Fig. 14 that showed that oxygen reduction on pyrite only occurs at potentials below 0.5V.

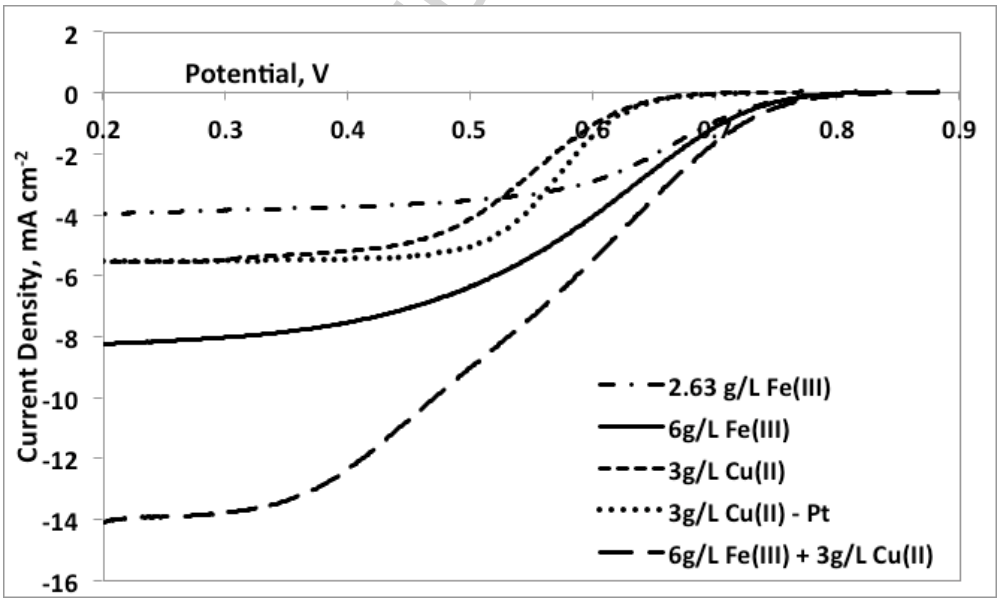

Fig. 15. Voltammograms (1mV/s) of a rotating (100 rev/min) pyrite1 electrode in a solution of 4M NaCl at pH 1.1 containing various concentrations of iron(III) and copper(II) at 35°C. The sweeps were initiated in a negative direction after 30 min at the rest potentials. Also shown is a curve for a rotating Pt electrode.

The limiting current densities calculated from the Levich equation are compared with the observed values in Table I.

Table I Observed and Calculated Limiting Currents

Solution	**i_L (obs)**	**i_L (calc)**
	mA cm^{-2}	**mA cm^{-2}**
3 g/L Cu(II)	5.5	5.6
6 g/L Fe(III)	8.4	8.7
3 g/L Cu(II) + 6 g/L Fe(III)	14.2	14.3

The good agreement of these values confirms that the currents measured are due to the reduction of the metal ions with negligible contribution from reduction of pyrite in this potential region.

Similar results in the region of the mixed potential were obtained in 1M HCl solution as shown in Fig. 16 for iron(III) with similar curves for copper(II). Extrapolation of a Tafel plot of the data for 1 g/L iron(III) to the mixed potential gave an estimate of the rate of dissolution (1-e basis) of 0.032 mA/cm^2 that is some 30 times that for dissolution in the presence of oxygen. This serves to highlight the fact that, as in the case of most sulfide minerals, oxygen is a poor oxidant compared to iron(III) in acid solutions.

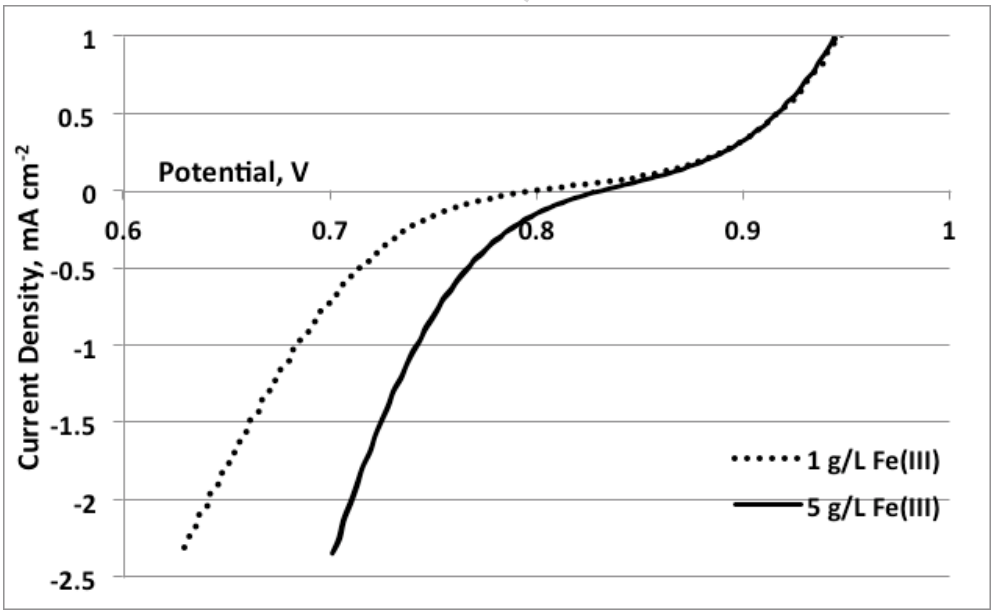

Fig. 16. Voltammograms (1mV/s) of a rotating (100 rev/min) pyrite1 electrode in a solution of 1M HCl containing iron(III) at 35^{o}C. The sweeps were initiated in a negative direction after 30 min at the rest potentials and only the positive-going sweeps are shown.

As pointed out in a recent publication (Nicol et al, 2016), it is not generally appreciated that the degree of agitation can, in some cases, have an effect on the cathodic (or anodic) currents at

potentials which are close to the equilibrium (or mixed) potential i.e. at current densities that are very much lower than the limiting current density for the reduction of an oxidant such as copper(II) or iron(III). This will occur in cases for which the rates of reduction are relatively high such as observed with pyrite. Measurements with pyrite showed that the current density appeared to vary with agitation even at potentials very close to the mixed potential. In fact, the mixed potential itself increases with increased rotation speed of the electrode as shown in Fig. 2 and Fig. 3. A similar effect was observed in a sulfate system but not explained in a recent publication (Nicol et al, 2013). Potentiostatic measurements were therefore made at potentials close to the mixed potentials on pyrite electrodes in a solutions of iron(III), copper(II) and a mixture of both in 4M NaCl. The electrode was rotated at various speeds and the steady current densities measured as shown in Fig.17 in the case of iron(III).

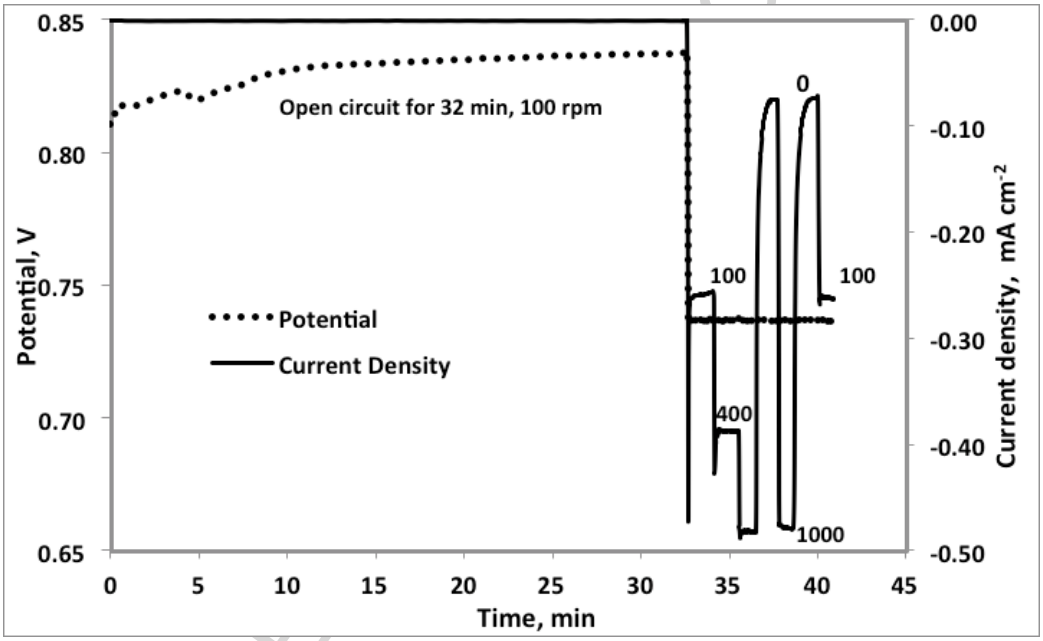

Fig. 17. Effect of rotation speed on reduction of iron(III) at 0.74 V in a solution of 6 g/L Fe(III) in 4M NaCl at pH 1.1 and 25°C after 32 min open circuit. The figures adjacent to the plot are the rotation speed (rev/min) of the electrode.

The results are plotted in Figs 18 and 19 as the reciprocal of the current density versus the reciprocal of the square root of the rotation speed. This linear relationship is predicted (Nicol et al, 2016) under conditions such that the current density is very much less than the limiting current density for the reduction of copper(II) or iron(III).

The origin of this effect in the case of copper(II) for example is that the reverse reaction of anodic oxidation of copper(I) occurs simultaneously with the cathodic reduction of copper(II) at these potentials and the rates of each are equal at the equilibrium potential. In this case, copper(I) is not present in the bulk of the solution but is produced by reduction of copper(II) at the surface

of the electrode. As the rotation speed increases, this copper(I) is removed more rapidly from the surface of the electrode and the anodic current for oxidation of copper(I) is thereby diminished with a resulting increased net cathodic current. Similar considerations apply to the reduction of iron(III).

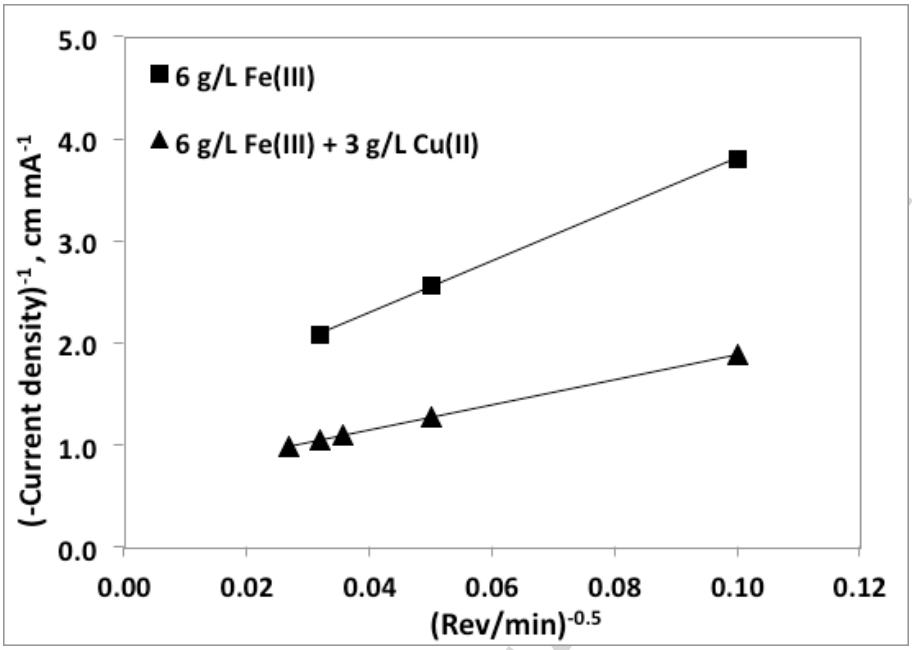

Fig. 18. Variation of cathodic current density at 0.74V with rotation speed of pyrite1 electrode in 4 M NaCl at pH 1.1 at 25^{o}C. Also shown is the data for a solution also containing 3 g/L copper(II).

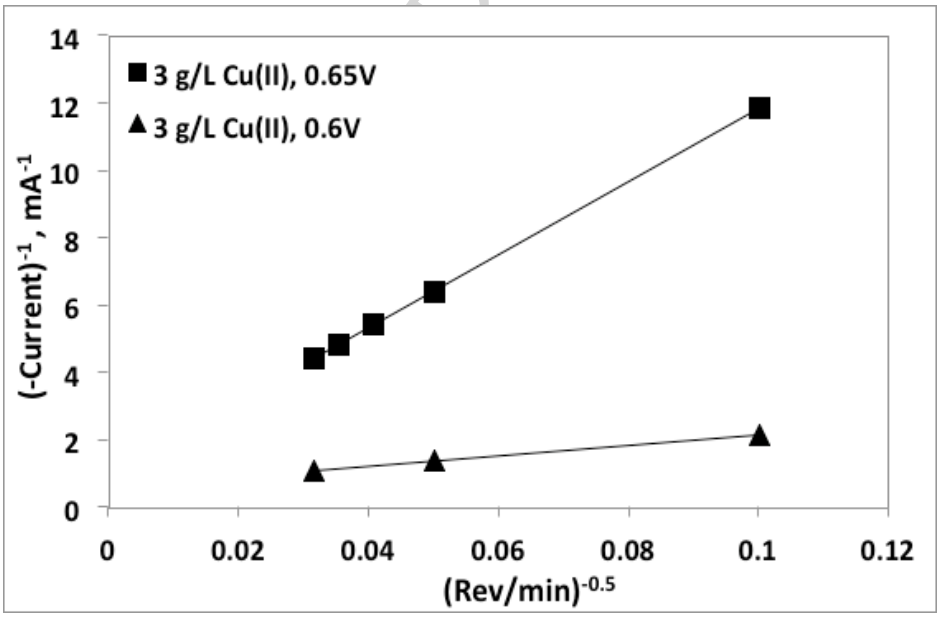

Fig. 19. Effect of electrode rotation speed on the steady-state cathodic current at fixed potentials for a pyrite1 electrode in a solution of 4M NaCl + 3 g/L Cu(II) at pH 1.1.

Extrapolation of these plots to infinite rotation, i.e. $(1/i)^{0.5} = 0$, gives the current due to the reduction of copper(II) or iron(III). Table II summarizes these estimated current densities for the reduction of copper(II) and iron(III)

Table II Estimated Current Densities for Reduction of Copper(II) and Iron(III)

	mA cm^{-2}		
	0.60V	**0.65V**	**0.74V**
3 g/L Cu(II)	3.81	2.38	0.78
6 g/L Fe(III)			0.77
Cu(II) + Fe(III)			1.49

These results show that at the same potential, copper(II) reduction occurs at about the same rate as iron(III) and that the rate of reduction of a mixture of copper(II) and iron(III) can be considered as being simply the sum of the individual currents.

4. Comparison with Chalcopyrite

The rate of dissolution of pyrite in solutions containing iron(III) or copper(II) can (in terms of the mixed potential model) be estimated by reading the current density measured in a solution without oxidant at the mixed potential measured in a solution with oxidant.

Thus, using the two solutions shown in Table 2, the mixed potentials in these solutions containing the oxidant mixture shown can be measured for both minerals. Then the solution is replaced by solutions of the same composition without the oxidant mixture and the current densities at the previously determined mixed potentials monitored as a function of time for both minerals. The current density (i_{diss}) after 60 min can then be considered as proportional to the rate of dissolution. A comparison of the rates estimated in this manner is given in Table III.

Table III Comparative Rates of Dissolution of Chalcopyrite and Pyrite at 25°C

Mineral	**Solution**	**Oxidant 1**		**Oxidant 2**	
		E_m V	**i_{diss} uAcm^{-2}**	**E_m V**	**i_{diss} uAcm^{-2}**
Pyrite	4M NaCl, pH 1	0.694	1.0	0.751	4.5
Chalcopyrite*	4M NaCl, pH 1	0.691	8.4	0.717	11.2

Oxidant 1: 1.8 g/L iron(III), 1.6 g/L iron(II) and 0.5 g/L copper(II), E_H = 0.693V
Oxidant 2: 1.8 g/L iron(III), 0.16 g/L iron(II) and 0.5 g/L copper(II), E_H = 0.751V
* Nicol and Zhang, 2017

These results confirm the above that the rate of pyrite dissolution is significantly slower than that of chalcopyrite under the same conditions, particularly at low potentials. Also, as shown in Fig. 6, the production of sulfate ions (required to generate heat in a heap leach process) by oxidation of pyrite is unlikely to be significant at potentials below 0.8V that are typical of heap leaching in chloride solutions. Thus, based on these considerations, generation of heat by oxidation of pyrite during heap leaching in chloride solutions cannot be expected.

5. Conclusions

This detailed study of the electrochemical behaviour of natural pyrite in acidic chloride solutions should be considered in conjunction with the previous paper (Nicol et al, 2016) on the cathodic reactions of copper(II) and iron(III) and the main conclusions can be summarized as follows.

The stoichiometry of the anodic dissolution reaction depends on the potential in that it varies from less than 4F/mole Fe dissolved at potentials below 0.8V to 15F/mole Fe at potentials above about 1.0V. It is not possible on the basis of this data to conclude whether this variability is a result of parallel or series reactions.

The mixed potentials of pyrite in chloride solutions containing iron(III) are greater than those in the presence of copper(II) and both increase with agitation as a result of enhanced transport of iron(II) and copper(I) from the surface of the dissolving mineral. The mixed potentials are unaffected by the presence of dissolved oxygen confirming the low reactivity for the cathodic reduction of oxygen.

The rate of anodic dissolution of pyrite in chloride solutions is independent of the acid and chloride concentration except at high chloride concentrations when the rate decreases slightly. The potential dependence of the anodic reaction roughly follows Tafel behaviour up to about 1.0V but mechanistic conclusions are excluded due to the variable stoichiometry.

Cathodic reduction of oxygen is some 30 times slower than that of 1 g/L iron(III) and that of copper(II) is also less significant in the leaching of pyrite due to the lower formal potential of the copper(II)/copper(I) couple than that of the iron(III)/iron(II) couple in concentrated chloride solutions.

Comparative measurements have shown that pyrite will dissolve more slowly than chalcopyrite in chloride solutions and, this coupled to the low sulfate yield at low potentials, suggests that oxidation of pyrite as a source of heat in abiotic heap leaching is unlikely.

6. References

Ahlberg, E. and Broo, A. E. Electrochemical reaction mechanisms at pyrite in acidic perchlorate solutions. *J. Electrochem. Soc*. **144**, 1997, 1281-1286.

Antonijevic, M. M.; Dimitrijevic, M. D.; Serbula, S. M.; Dimitrijevic, V. L. J.; Bogdanovic, G. D.; Milic, S. M. Influence of inorganic anions on electrochemical behaviour of pyrite. *Electrochim. Acta*. **50**, 2005, 4160-4167

Aroca, F., Plant description and operation of heap leaching, solvent extraction, and electrowinning of copper at Minera Michilla. In: Jergensen, G. V. (Ed.), Copper Leaching, Solvent Extraction, and Electrowinning Technology, *Society for Mining, Metallurgy, and Exploration*, Littleton, Colorado, 1999, pp. 279-294.

Biegler T., Rand D.A.J. and Woods R. Oxygen reduction on sulfide minerals. Part 1. Kinetics and mechanism at rotated pyrite electrodes. *Electroanal. Chem. Interfac. Electrochem*. **60**, 1975. 151-162

Biegler, T. and Swift, D. A. Anodic behavior of pyrite in acid solutions. *Electrochim. Acta*. **24**, 1979. 415-20.

Bryson L.J. and Crundwell, F.K. The anodic dissolution of pyrite (FeS2) in hydrochloric acid solutions. *Hydrometallurgy*. **143**, 2014, 42-63

Holmes P.R. and Crundwell F.K. The kinetics of the oxidation of pyrite by ferric ions and dissolved oxygen: An electrochemical study. *Geochim. Cosmochim. Acta*. **64**, 2000, 263-274

Holmes, P. R.; Crundwell, F. K. Polysulfides do not cause passivation: Results from the dissolution of pyrite and implications for other sulfide minerals. *Hydrometallurgy.* **139**, 2013. 101-110.

Kelsall G.H., Yin Q., Vaughan D.J. and England K.E.R. Electrochemical oxidation of pyrite (FeS_2) in acidic aqueous electrolytes. In *Electrochemistry in Mineral and Metal Processing IV* (eds. F.M.Doyle, P.E.Richardson and R.Woods). The Electrochemical Society. 1996, 131-142

Lehmann, M. N., Stichnoth, M., Walton, D. and Bailey, S. I. The effect of chloride ions on the ambient electrochemistry of pyrite oxidation in acid media. *J. Electrochem. Soc*. **147**, 2000. 263-3271

Lehner, S., Savage, K., Ciobanu, M. and Cliffel, D. E. The effect of As, Co, and Ni impurities on pyrite oxidation kinetics: An electrochemical study of synthetic pyrite. *Geochim. Cosmochim. Acta* **71**, 2007. 2491-2509.

Lin, H. K. and Say, W. C. Electrochemical study of pyrite oxidation in chloride solution. *EPD Congress 1997*, (ed. Brajendra. M.). Proceedings of Sessions and Symposia TMS Annual Meeting, Orlando, Fla., 1997. 149-165.

Lin, S., Liu, Q. and Li, H. Electrochemical behavior of pyrite in acidic solution with different concentrations of NaCl. *Chin. J. Geochem*. **33**, 2014, 374-381.

Martell, A.E. and Smith, R.M., NIST Standard Reference Database 46, Ver 8. National Institute of Standards and Technology, Gaithersburg, MD, USA, 2004.

Miki, H. and Nicol, M.J. The kinetics of the copper-catalysed oxidation of iron(II) in chloride solutions. In: Young, C., Anderson, C., Taylor, P., Choi, Y. (eds.), *Hydrometallurgy 2008*, The Minerals, Metals and Materials Society, Warrendale, PA, USA, 2008, 971-979.

Miki, H and Nicol, M.J., Synergism in the oxidation of covellite and pyrite in chloride solutions containing iron(III) and copper(II). In: Young, C., Anderson, C., Taylor, P., Choi, Y. (eds.),

Hydrometallurgy 2008, The Minerals, Metals and Materials Society, Warrendale, PA, USA, 2008, 646-652.

Miki, H. and Nicol, M.J. The dissolution of chalcopyrite in chloride solutions. Part 4. The kinetics of the auto-oxidation of copper(I). *Hydrometallurgy*. **105**, 2011. 246-250.

Misra, K.K. and Osseoasare, K. Aspects of the interfacial electrochemistry of semiconductor pyrite (FeS_2). *J. Electrochem. Soc*. **135**, 1988, 2502-2509

Misra, K.K. and Osseoasare, K. Electroreduction of Fe^{3+}, O_2 and $Fe(CN)_6^{3-}$ at the n-pyrite (FeS_2) surface. *J. Electrochem. Soc*. **139**, 1992, 3116-3120

Nicol, M.J. and Lazaro, I. The role of Eh measurements in the interpretation of the kinetics and mechanisms of the oxidation and leaching of sulfide minerals. *Hydrometallurgy*, **63**, 2002, 15-22

Nicol, M.J. and Liu, J.Q. The effect of chloride ions on the oxidation of pyrite under pressure oxidation conditions. *Hydrometallurgy 2003*, The Minerals, Metals and Materials Society, Warrendale, Pennsylvania, **1**, 2003, 591-602

Nicol, M., Miki, H., Zhang, S. and Basson, P. The effects of sulfate ions and temperature on the leaching of pyrite. 1. Electrochemistry. *Hydrometallurgy*, **133**, 2013. 88-196.

Nicol, M.J., Tjandrawan, V. and Zhang, S. Cathodic reduction of iron(III) and copper(II) on various sulfide minerals in chloride solutions. *Hydrometallurgy* **166**, 2016, 113-122.

Nicol, M.J. and Zhang, S. The anodic behaviour of chalcopyrite in chloride solutions: Potentiostatic measurements. *Hydrometallurgy*, **167**, 2017, 72-80.

Peters, E. and Majime, H. Electrochemical reactions of pyrite in acidic perchlorate solutions. *Can. Metall. Q*. **7**, 1968, 111-117

Rimstidt, J. D. and Vaughan, D. J. Pyrite oxidation: a state-of-the-art assessment of the reaction mechanism. *Geochim. Cosmochim. Acta* **67**, 2003, 873-880.

Vogel, A.I. A Textbook of Quantitative Inorganic Analysis, 3rd Edition, Longman, London, 1961, p 787.

Zhu, X., Li, J., Bodily, D.M. and Wadsworth, M. E. Transpassive oxidation of pyrite. *J. Electrochem. Soc*. **140**, 1993. 1927-35.

Highlights

- The stoichiometry of dissolution varies from less than 4F/mole Fe at low potentials to 15F/mole Fe at potentials above 1.0V.
- Mixed potentials increase with agitation as a result of enhanced transport of iron(II) and copper(I) from the surface.

- The rate of anodic dissolution of pyrite in chloride solutions is independent of the acid and chloride concentration
- The potential dependence of the anodic reaction roughly follows Tafel behaviour up to about 1.0V
- Cathodic reduction of oxygen is some 30 times slower than that of 1 g/L iron(III)
- Pyrite will dissolve more slowly than chalcopyrite in chloride solutions